



## **ON SEISMIC BEHAVIOR OF A 130M HIGH ROCKFILL DAM: AN INTEGRATED APPROACH**

**Anastasios ANASTASIADIS<sup>1</sup>, Nikolaos KLIMIS<sup>1</sup>, Konstantia MAKRA<sup>1</sup> and Basil MARGARIS<sup>1</sup>**

### **SUMMARY**

The present work focuses on a comprehensive exploration of seismic behavior of a central clay core rockfill dam subjected to strong input motion. The 130m high dam is to be constructed at a moderate seismic zone of Northern Greece, resting on limestones and phyllites. An integrated seismological, geophysical and geotechnical approach is used to investigate the response of the above dam during the Safety Evaluation Earthquake (SEE). Dynamic analysis of the examined dam is based on a 2-D finite element mesh in three different cross sections, where cyclic soil behavior is simulated using equivalent linear model. The input motion used for dynamic analyses results from four different accelerograms, registered at different sites with horizontal peak acceleration scaled at 0.37g, thus corresponding to SEE (mean return period of  $T=10000$  years), according to Swiss and US earthquake guidelines for dams. Results are presented and discussed with special emphasis on the effect of non-linear soil behavior and frequency content of seismic excitations. Anelastic displacements are calculated decoupled to the aforementioned methodology representing a basic criterion of seismic sufficiency for the examined dam. Decoupled seismic response analyses revealed that shallow slides could move up to 1.3m or 1.5m in a worst case scenario, whereas for deeper slides, maximum permanent displacements are expected to be less than 1m, during S.E.E. Therefore, potential reduction of freeboard and danger of internal erosion are lower than safety limits proposed by Swiss Seismic Guidelines.

### **INTRODUCTION**

Procedures used to evaluate the seismic safety of earth and rockfill dams have evolved gradually over the last 40 years. Until early sixties, the pseudostatic approach represented the unique tool used to assess the seismic safety of most geotechnical structures (dams and embankments included). Nowadays, this method is still in wide use (Wieland [1], Cascone [2]) because several national regulations are based on it and also because geotechnical engineers are confident in its use.

Displacement-based approaches provide a compromise between the pseudostatic approach and the more refined numerical analyses. Reliable numerical analyses require accurate evaluation of soil profile, initial

---

<sup>1</sup> Researcher, Institute of Engineering Seismology & Earthquake Engineering (ITSAK), 46, Georgikis Scholis str., P.O. Box 53, GR-55102, Finikas, Thessaloniki, GREECE ([anastas@itsak.gr](mailto:anastas@itsak.gr), [klimis@itsak.gr](mailto:klimis@itsak.gr), [makra@itsak.gr](mailto:makra@itsak.gr), [margaris@itsak.gr](mailto:margaris@itsak.gr))

stress state and stress history, pore water pressure conditions, whereas cyclic soil behavior need the use of advanced constitutive models developed within the framework of bounding surface plasticity or kinematic hardening plasticity, thus requiring input parameters not usually measured in field and conventional laboratory testing.

In this work, the seismic stability of a clay core rockfill dam has been studied by decoupling the dynamic response analysis from the sliding block analysis. The geotechnical characterization of the earth dam and the foundation soils allowed prescribing the design parameters for the computation of the dynamic response of the dam. Real accelerograms, yet modified to account for the desired peak ground acceleration, were used as input motions. The results of the analysis showed that different patterns of dynamic behavior could be obtained depending on the characteristics of the assumed input motions, thus indicating the need to obtain a significant range of possible dam responses. This prerequisite was achieved, besides the assignment of excitations motions with different frequency characteristics, with a parametric analysis on dynamic characteristics of dam shell and rockfill cover. Dynamic response of the dam was evaluated using a 2D finite element method while the earthquake-induced displacements were evaluated using the sliding block analysis method, following the procedure described in Makdisi [3] and a modified version of Newmark's method [4].

## SITE DESCRIPTION AND GEOTECHNICAL CHARACTERIZATION

This central clay core rockfill dam is going to be constructed in Western Macedonia, Northern Greece. A brief geological map of the site is given in figure 1 while figure 2 shows in detail the highest cross-section of the dam; the crest is 564m long, 15m wide and 130m high above the foundation level with a freeboard of 7.0m. Upstream and downstream slopes have an inclination of 1:2.25 (vertical:horizontal) and 1:2 respectively, while slope inclination of the core is 5:1 (v:h) from both sides. The shells are covered by rockfill material also protected by a thin layer of rip-rap upstream and a thin layer of limestone cobbles downstream. The dam is mainly seated on phyllites· a smaller part of it is seated on limestones. In between these rock formations, there is a transition zone formed due to overthrust of limestone on phyllites. The upstream part of the dam's cross section (figure 2), is seated on alluvial deposits of variable thickness (max of 15m). Excavations of 10 to 20m under the core will precede the construction of the dam in order to remove soil deposits as well as the weathered zones of the rock formations. A grout curtain extending into the lower rock formation prevents seepage through the alluvial deposits and weathered limestone or phyllite.

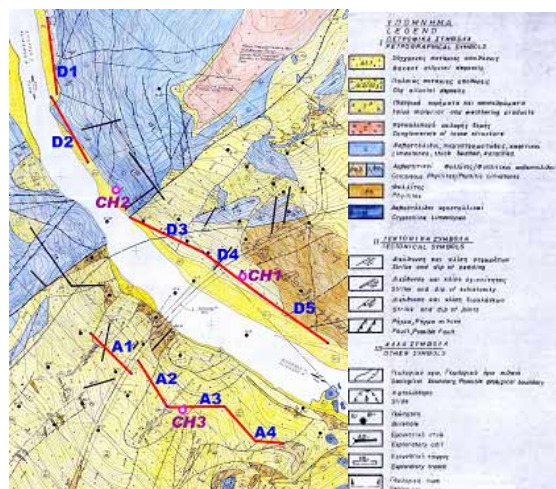


**Figure 1. Geological map of the area showing site of in situ measurements (Cross holes: CH1, CH2, CH3, Refraction seismic lines: A1 to A4 and D1 to D5)**

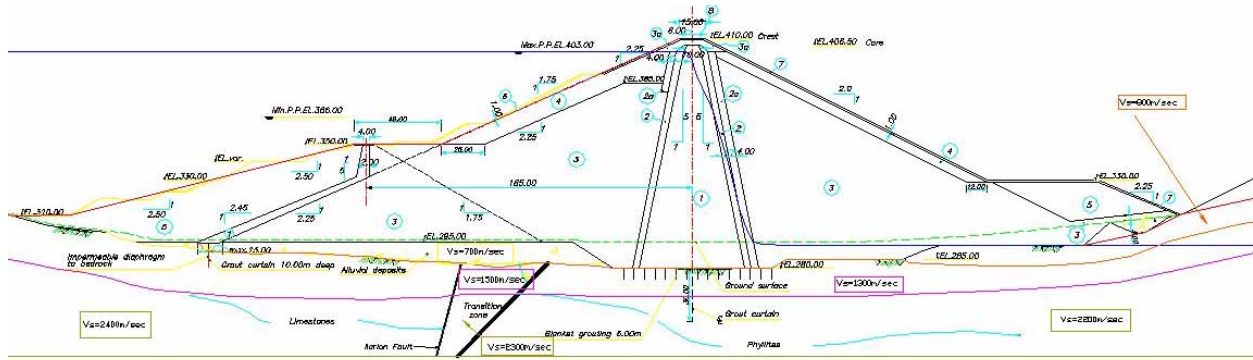


**Figure 2. Central Cross-section of the dam**

To study the dynamic response of the dam, a reliable set of stiffness, strength and damping properties are necessary, thus a detailed as possible geotechnical investigation (assignment of dynamic properties) of foundation soils/rocks as well as of the materials filling the dam (shells, rockfill, weathered phyllite from required excavations) were performed. The geotechnical investigation consisted of both in-situ measurements and laboratory tests. Specifically, three Cross-Hole tests were carried out as well as nine seismic refraction lines were deployed in order to determine the P and S wave velocities of the rock formations. The positions of the in-situ measurements are depicted in figure 1. The results from the in-situ measurements were carefully evaluated and combined in order to give the design parameters, indicating that limestone is separated in two layers with a clear difference in the Vs values of these layers, whereas phyllites consist of three zones. Analogously to limestone formation, the transition zone between limestone and phyllites is separated in two layers. Vs values and thickness for each layer are given in Table 1.

**Table 1. Shear wave velocities and thicknesses of foundation rock formations of the dam**

	Limestone		Transition zone		Phyllites	
	Vs (m/sec)	Thickness (m)	Vs (m/sec)	Thickness (m)	Vs (m/sec)	Thickness (m)
1 <sup>st</sup> layer (surface)	1700	25	1500	16-17	800	11-14
2 <sup>nd</sup> layer	2400	bedrock	2300	bedrock	1300	14-21
3 <sup>rd</sup> layer					2200	bedrock

Laboratory tests were performed on soil samples of clay that will be used to construct the core and sand-gravel mixtures of the main body (shells and rockfill) of the dam. Specifically, six clayey samples were remolded and compacted to fit actual conditions after the construction of the dam. Three of them were tested in Resonant Column Apparatus, while the rest on the Cyclic Triaxial Apparatus to determine both the maximum shear modulus and the dependence of its normalized value as well as damping on a wide range of deformations ( $10^{-4}$  to 3%). In addition to the above, six samples of sand-gravel mixture (river alluvium) intended to be used for the shell of the dam were remolded and compacted and then tested under undrained conditions on the Cyclic Triaxial Apparatus in order to define their resistance against liquefaction. The tested sand-gravel mixture is representative of the material aimed to be used for the construction of the dam shells at the only difference that particles exceeding 19mm were excluded. The samples tested were highly compacted exhibiting a relative density,  $Dr=87-89\%$  and a void ratio,  $e=0.22-0.23$ . During CTX tests, no liquefaction sign occurred, even for a very high number of loading-unloading cycles ( $N=200$ ). A number of 15 cycles corresponds to the analogous effect of an earthquake of magnitude  $M=7.5$  (Gazetas [5]). The ratio of pore pressure build-up for 15 cycles over the effective confinement pressure  $\Delta u / \sigma'_3$  was measured almost 0.15, far below the limit of 0.6 to 0.7 considered as the threshold of liquefaction (Das [6], Seed [7]).

Table 2 summarizes soil materials used to construct different parts of the dam (figure 3), as well as the alluvial layer on which the dam is seated. In the same table, the relationships providing the maximum shear modulus,  $G_o$ , as a function of mean effective stress  $\sigma'_o$  for each material are adopted after careful evaluation of performed laboratory tests with other available results from the international literature. To evaluate the low-strain shear modulus in the dam and in foundation soils through the equations of table 2, the initial state of effective stress was obtained from a static 2-D numerical analysis in which the dam's multistage construction and the reservoir impoundment were modeled, whereas seepage line was imposed via decoupled hydraulic analysis. The resulted low strain shear wave velocity distribution over the main cross-section of the dam is given in Figure 4. Figures 5 to 7 show the dependency of soil stiffness and damping on strain level that were assigned to soil and rock materials based on both results from RC and CTX tests and literature information.

**Table 2. Soil description & shear modulus relationships for the construction materials of the dam**

	Soil description	$G_o = f(\sigma'_o)$	Vs (m/sec)	
			Min	max
Core	Low plasticity sandy clayey silt (CL)	$G_o = 7304\sigma'^{0.58}_o$	205	405
Shell	Sand-Gravel mixture (e=0.30)	$G_o = 14.731\sigma'^{0.62}_o$	205	840
Rockfill	Sand-Gravel mixture (e=0.40)	$G_o = 12.255\sigma'^{0.62}_o$	270	380
Fill	Weathered phyllites from excavations (gravelous mixture with pebbles)	$G_o = 15\sigma'^{0.50}_o$	185	400
Alluvial	Alluvial river deposits (sands, clays, gravels, pebbles)	$G_o = 17\sigma'^{0.50}_o$	350	520

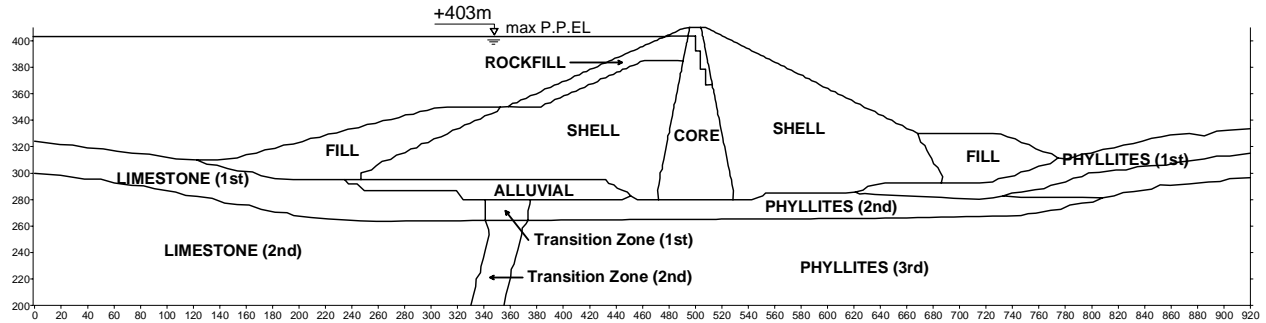


**Figure 3. Correspondence of materials (Table 1 and 2) with different parts of the dam**

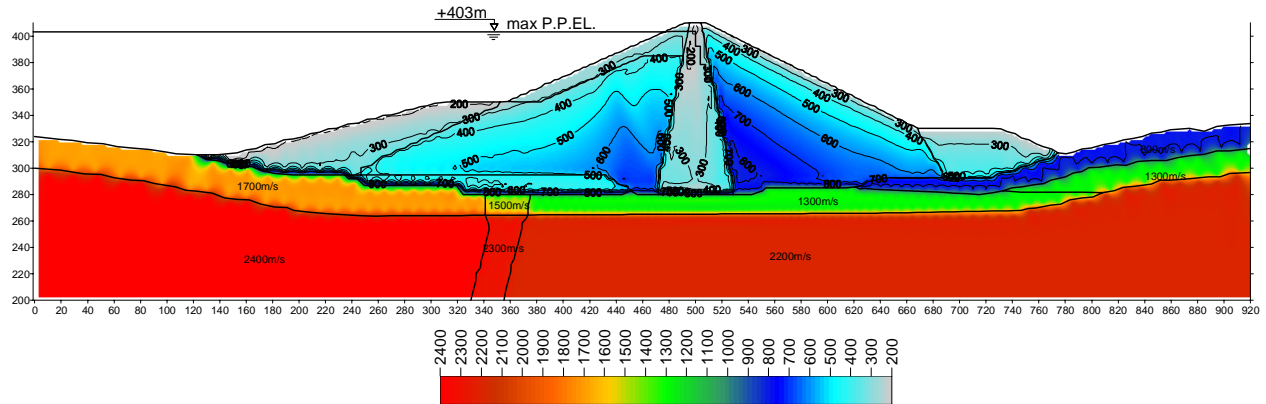


**Figure 4. Shear wave velocity distribution along the main cross-section of the dam**

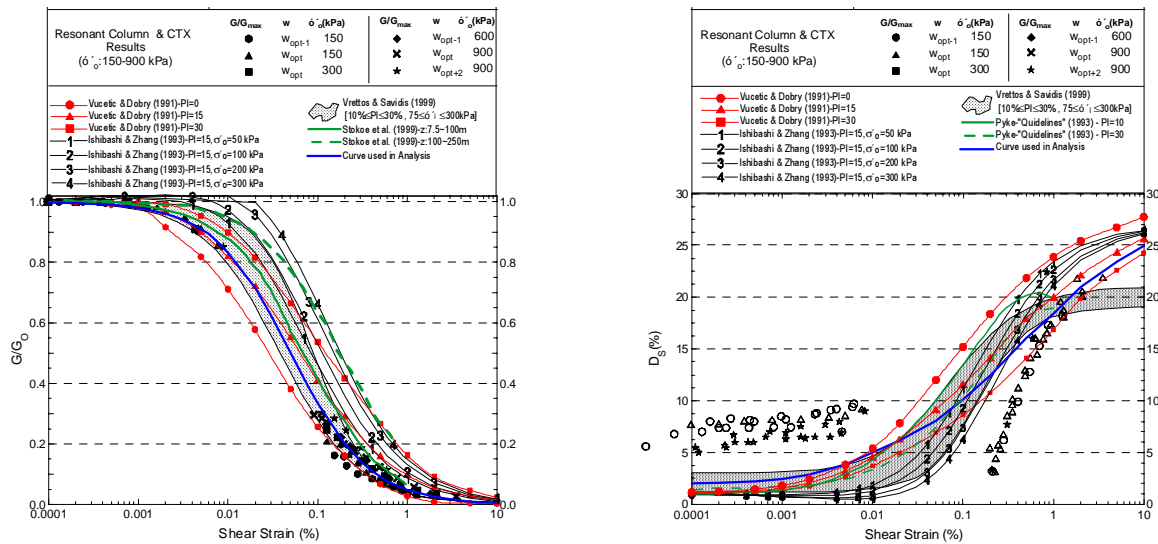


**Figure 5. Normalized shear modulus (left) and damping ratio (right) against shear strain for the clayey material of the dam core.**

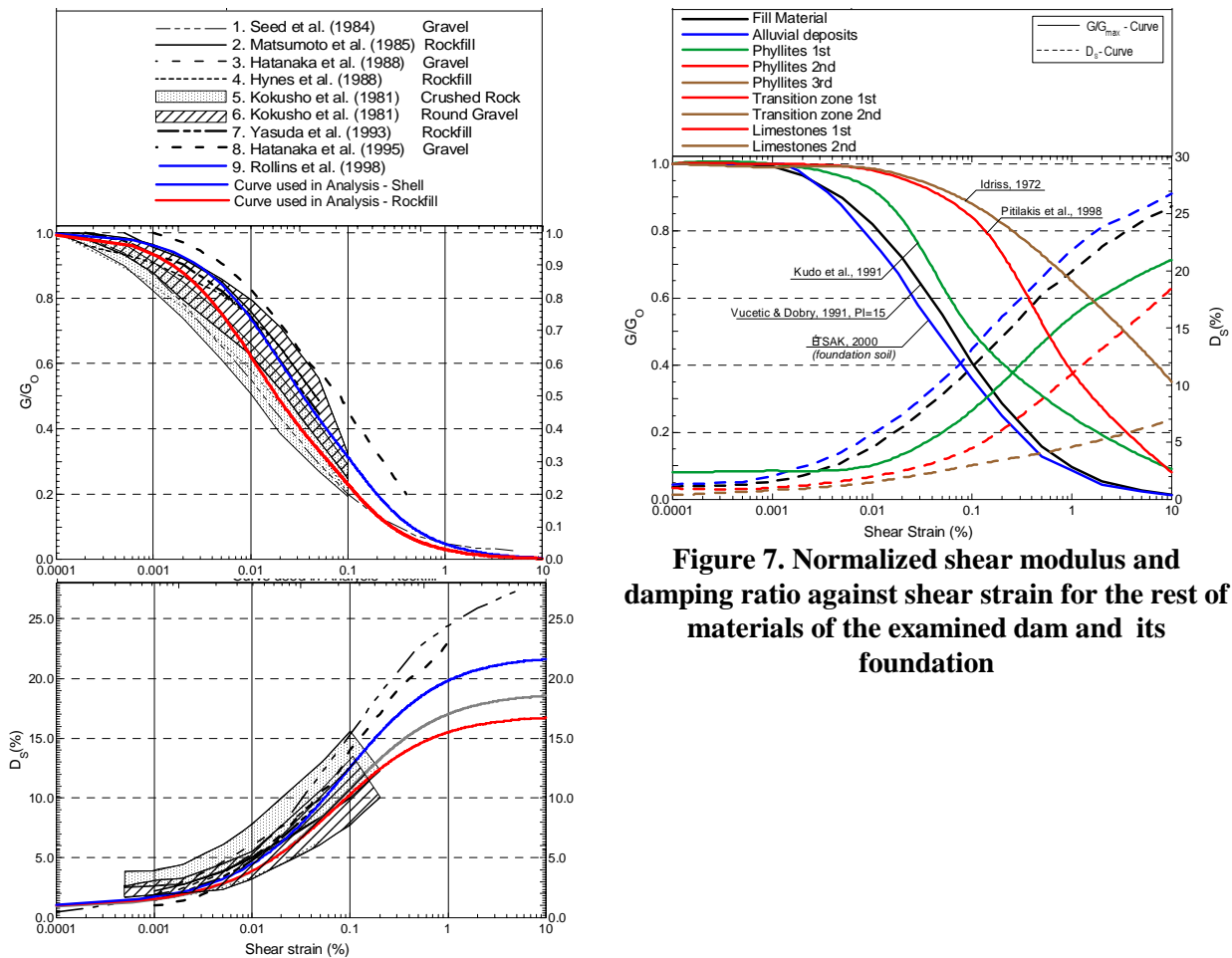


**Figure 6. Normalized shear modulus (up) and damping ratio (down) against shear strain for the material of the dam shell and rockfill.**

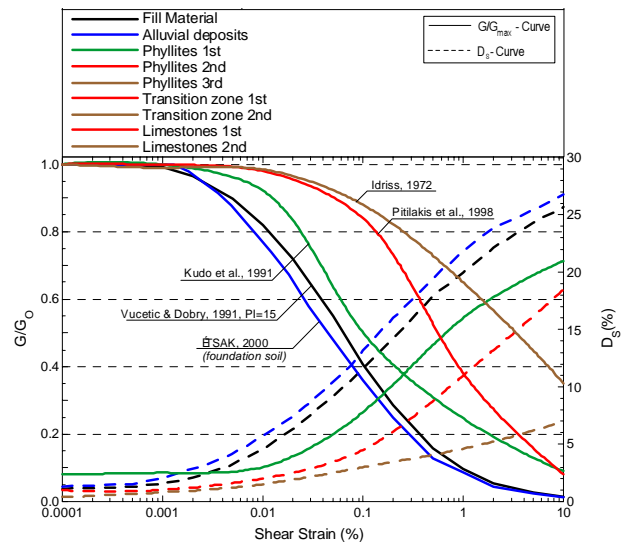


**Figure 7. Normalized shear modulus and damping ratio against shear strain for the rest of materials of the examined dam and its foundation**

## INPUT MOTION

Assessment of the seismic stability of dams requires preliminary specification of input ground motion that generally involves seismic hazard analysis and ground response analysis. According to recent Swiss Guidelines for the aseismic design of dams [8], earth or rockfill dams higher than 40m belong to category I, and they are studied for the Safety Evaluation Earthquake (SEE) with 1% probability of exceedance over a period of 100 years, namely for an earthquake with a mean return period of 10000 years (Finn [9], [10]). Based on seismicity and seismic hazard studies for the area under consideration, the average expected peak ground horizontal acceleration for an earthquake with mean return period of 10000 years and outcrop rock conditions is estimated at 0.37g.

For the seismic stability of this dam, four real accelerograms were considered in the analyses (Table 3). They were selected to satisfy the following criteria: a) originated from earthquakes that have similar seismotectonic environment to that of the area under study, b) recorded at rock outcrop sites (if possible), c) at different epicentral distances to account for waveforms from near, intermediate and far field conditions and d) to cover the response spectra provided by the Greek seismic code (EAK [11]) and Eurocode 8 for soil type A, that is for rock or rock-like formations whose average shear wave velocity in the first 30m exceeds 800m/sec (EC8 [12]).

**Table 3. Seismological and site conditions information for the selected accelerograms**

No	Earthquake Name	Magnitude*	Epicentral Distance (km)*	Station Name	Soil class*	T <sub>m</sub> (sec)
1	Kozani (950513)	M 6.6	20	Prefecture	Rock	0.283
2	Aegio (950615)	Ms 6.2	18	OTE	deconvolved**	0.553
3	Valnerina (790919)	M 5.8	4	Cascia	Rock	0.269
4	Montenegro (790415)	M 7.04	65	Herceg Novi – O.S.	Rock	0.406

\* European Strong Motion Database (Ambraseys [13])

\*\* Personal communication with prof. G. Gazetas

Initial recorded peak ground accelerations range between 0.15 – 0.39g and thus they were scaled for the Safety Evaluation Earthquake at 0.37g. The frequency content of those records is characterized by the mean period T<sub>m</sub>, defined as

$$T_m = \frac{\sum_i C_i^2 (1/f_i)}{\sum_i C_i^2}$$

where C<sub>i</sub> are the square roots of the sum of the squared real and imaginary parts of the positive-frequency Fast Fourier Transform (FFT) coefficients, and f<sub>i</sub> are the discrete FFT frequencies from approximately 0.25 to 20Hz (Rathje [14]). The accelerograms used in the analyses are given in figure 8a, while figure 8b shows the comparison of their response spectra with those of EAK [10] and EC8 [11]. It is obvious that this set of records describe a wide range of frequencies that cover the whole period band of the plateau of the type A response spectrum (0.1-0.4sec), with the exception of that of the Aegio earthquake whose maximum spectral acceleration is observed at 0.553sec.

## RESPONSE ANALYSES OF DAM

The 2D response analyses of the dam were carried out using the FE code TELDYN [15]. It accounts for non-linear stress-strain and strain depended damping through the equivalent linear procedure. The real geometry of the dam and the foundation soil/rock formations were considered in the analysis. The FE



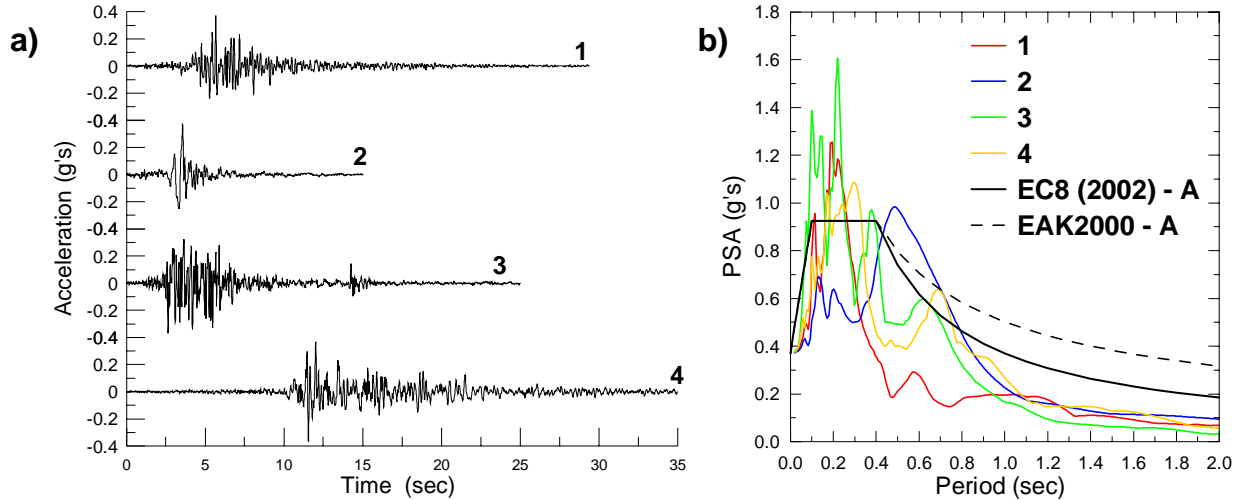


**Figure 8. a) Accelerograms used in the analyses, b) comparison of response spectra with those of soil type A proposed in EAK (2000) and EC8 (draft 2002).**

mesh for the cross-section of figure 2 consists of 3413 quadrilateral elements and extends 500 meters and 420m from the dam centre line towards the upstream and downstream directions respectively (figure 9). Shear wave velocities shown in figure 4 were used to compute  $G_{o,des}$  values for each element of the mesh. The scaled accelerograms described in the previous section were applied at the base of the mesh as input motions for the 2D response analyses. Synthetic accelerograms resulted from seismic wave propagation were obtained at several nodes of the mesh.

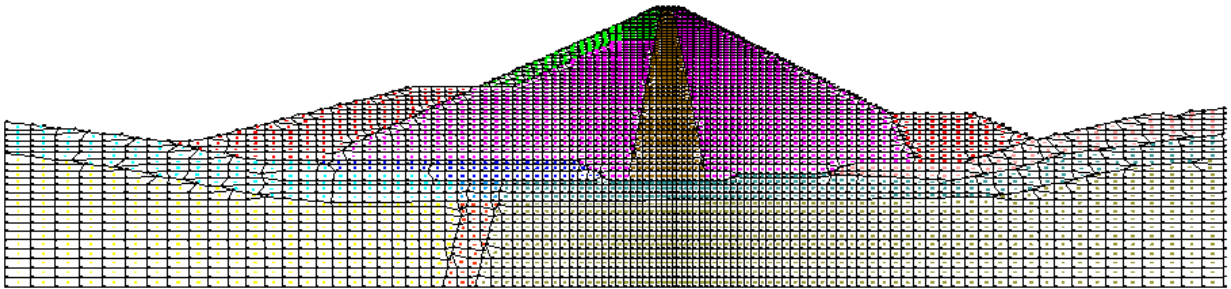


**Figure 9. FE mesh for the cross-section of figure 2.**

Typical contours of peak acceleration are given in figure 10 for Kozani (top) and Aegio (bottom) earthquake respectively (No 1 & 2 in table 3). Those cases were selected for illustration since they present the lowest and highest values of peak acceleration among the different analyses. In all cases, the major part of the dam's body is shaken by accelerations between 0.2 and 0.3g. Peak accelerations as high as 1.2g are obtained at a few to several meters depth at the side shells due to low confining stresses and in the proximity of the crest due to wave focusing effects. Consistently with peak accelerations, most of the soil mass undergoes effective strain levels lower than 0.1%, at the exception of zones described above where strain levels are as high as 0.3% at the side shells and might locally reach 1.0% inside the core of dam. The profiles of peak acceleration and effective shear strain obtained along the dam centre line are plotted in left and central part of figure 11. Peak accelerations do not vary significantly for depths larger than 40m and take values between 0.2 and 0.4g, while the maximum values attained at the crest are about twice the input peak acceleration with the exception of earthquake No 2 (Aegio) for which peak accelerations are three times higher. Shear strains increase with depth reaching values of 0.35% at almost 20m depth and gradually decreases to very low values down to a depth of 135m. At a small distance from the centre line

towards the upstream part of the dam, maximum effective shear strains are observed reaching values as high as 1.05% again at almost 20m depth.

In order to obtain a significant range of possible dam responses to account for its dependency on the characteristics of the input motion, different design assumptions have been investigated. Namely, parametric analyses on dam's response were performed assuming a 40% increase and a similar decrease

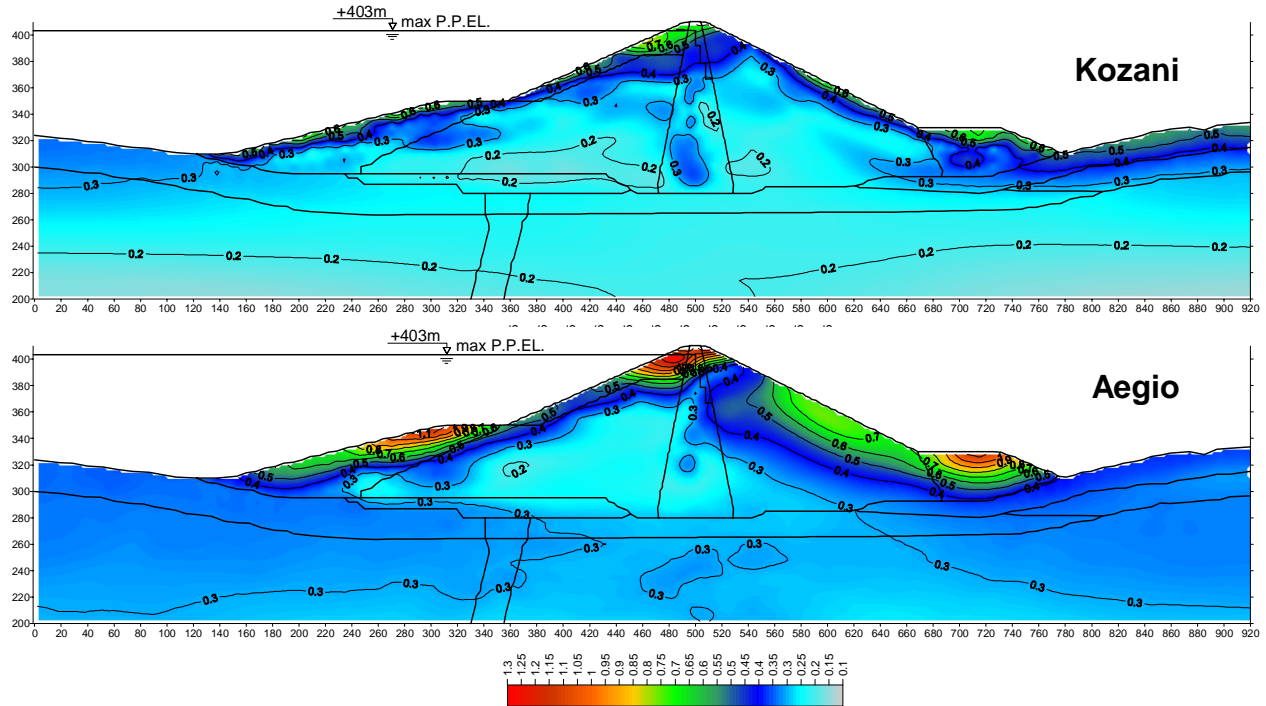


Figure 10. Typical contours of peak acceleration for Kozani (top) and Aegio (bottom) earthquake

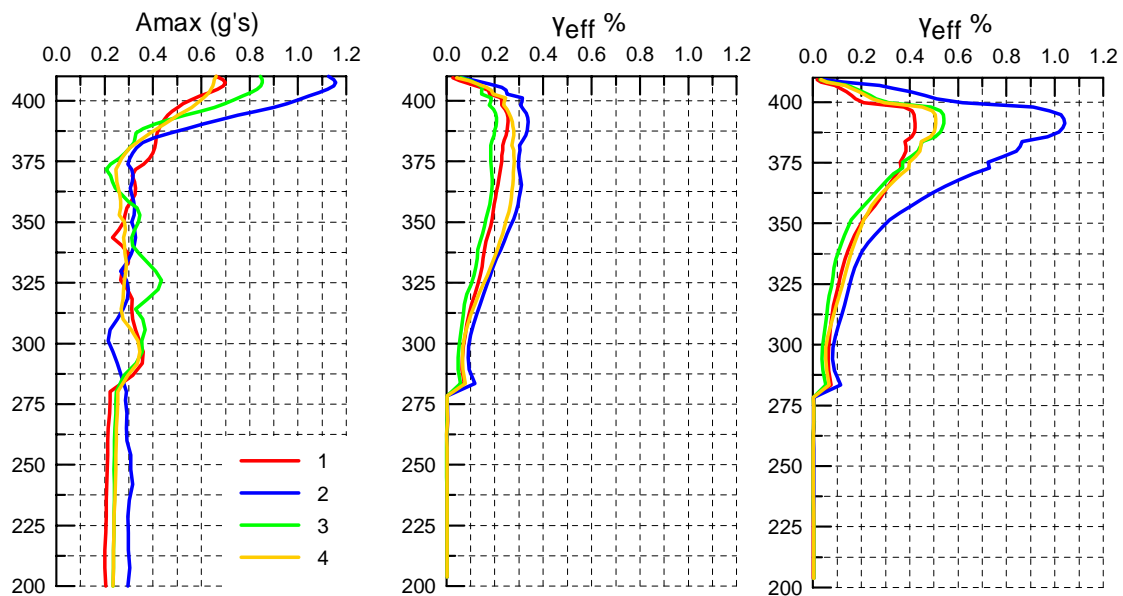


Figure 11. Profiles of maximum acceleration (left) and effective shear strain along the dam centre line (center) and at a small distance towards the upstream direction (right)



of maximum shear modulus of the shells and rockfill of the dam (from now on, referred as  $G_{o,max}$  and  $G_{o,min}$  analyses). For the foundation materials, a 20% change (increase or decrease on  $G_{o,des}$ ) was similarly adopted. Table 4 summarizes the different cases that have been studied in terms of the mean period of acceleration input motion,  $T_m$ , with respect to the fundamental period of the highest cross section of the dam,  $T_s$  for the design assumptions mentioned previously, together with values of peak acceleration and elastic displacements at the crest and the base of the dam. It is observed that the highest values of peak acceleration ( $\geq 1.0g$ ) and elastic displacements ( $>20cm$ ) at the crest are resulted from seismic analysis with earthquake No 2 independently of the assigned design parameters ( $G_{o,des}$ ,  $G_{o,max}$  and  $G_{o,min}$  cases). The ratio between the dam's fundamental period and mean period of No 2 input motion which ranges from 1.29 to 1.95 is close to resonance and thus results in large response parameters.

**Table 4. Mean period of acceleration input motion,  $T_m$ , and fundamental period of the dam's cross-section,  $T_s$ , together with values of peak acceleration and elastic displacements at the crest and the base of the dam for the cases of  $G_{o,des}$ ,  $G_{o,max}$  and  $G_{o,min}$  analyses**

	Earthq No	$T_m$ (sec)	$T_s$ (sec)	$T_s / T_m$	$a_{m,cr}$ (g)	$a_{m,b}$ (g)	$a_{m,o}$ (g)	$a_{m,cr}/a_{m,b}$	$a_{m,cr}/a_{m,o}$	$d_{m,cr}$ (cm)	$d_{m,b}$ (cm)
$G_{o,des}$	1	0.283	0.839	2.97	0.69	0.22	0.37	3.14	1.86	9.4	2.4
	2	0.553		1.52	1.15	0.29	0.37	3.97	3.11	24.0	10.9
	3	0.269		3.12	0.85	0.25	0.37	3.40	2.30	8.4	3.2
	4	0.406		2.07	0.65	0.25	0.37	2.60	1.76	11.5	5.1
$G_{o,max}$	1	0.283	0.713	2.52	0.67	0.22	0.37	3.05	1.81	5.79	2.52
	2	0.553		1.29	1.29	0.29	0.37	4.45	3.49	21.62	8.12
	3	0.269		2.65	0.74	0.25	0.37	2.96	2.00	7.73	3.07
	4	0.406		1.76	0.78	0.25	0.37	3.12	2.11	11.04	3.94
$G_{o,min}$	1	0.283	1.076	3.80	0.42	0.23	0.37	1.83	1.14	9.59	2.27
	2	0.553		1.95	1.00	0.29	0.37	3.45	2.70	28.38	17.25
	3	0.269		4.00	0.55	0.26	0.37	2.12	1.49	7.04	3.18
	4	0.406		2.65	0.56	0.26	0.37	2.15	1.51	13.97	6.62

$a_{m,cr}$  : peak crest acceleration

$d_{m,cr}$  : peak crest elastic displacement

$a_{m,b}$  : peak base acceleration

$d_{m,b}$  : peak base elastic displacement

$a_{m,o}$  : peak input acceleration (outcrop rock)

## PERMANENT DISPLACEMENTS

The seismic stability of this rockfill dam is expressed in terms of accumulated – during a seismic event – permanent displacements of a potential sliding mass and computed a posteriori (decoupled analysis) following firstly the simplified procedure proposed by Makdisi [3] and secondly on Newmark's [4] sliding block methodology.

The most critical slip surfaces and the corresponding yield accelerations,  $a_y$ , are necessary for the application of the aforementioned approaches. To evaluate yield acceleration and the associated sliding surface, a pseudostatic approach was used for a condition of incipient movement (factor of safety,  $F_s=1$ ) for both upstream and downstream slopes. Twelve slip surfaces were examined for the main cross section of figure 2, covering all possible cases, from shallow to deep slip surfaces, local to more extended ones passing through the shell in a considerable depth as well as through the core of the dam (figure 12). Pseudostatic analyses undertaken on either upstream and downstream sides of the dam, exhibited that

yield acceleration for the upstream slip surfaces range from 0.134 to 0.253g, while for downstream ones from 0.273 to 0.313g (Table 5). The above pseudostatic analyses were performed for undrained conditions for the clayey ore of the dam (with a reduction of about 15% to 20% of the undrained shear strength as measure from monotonic test in order to account for cyclic behavior) and with effective characteristics for the shells and upstream rockfill of the dam. The internal angle of friction of the upstream shell has been adequately reduced in order to account for the pore pressure build-up according to EAK (2000) suggestions.

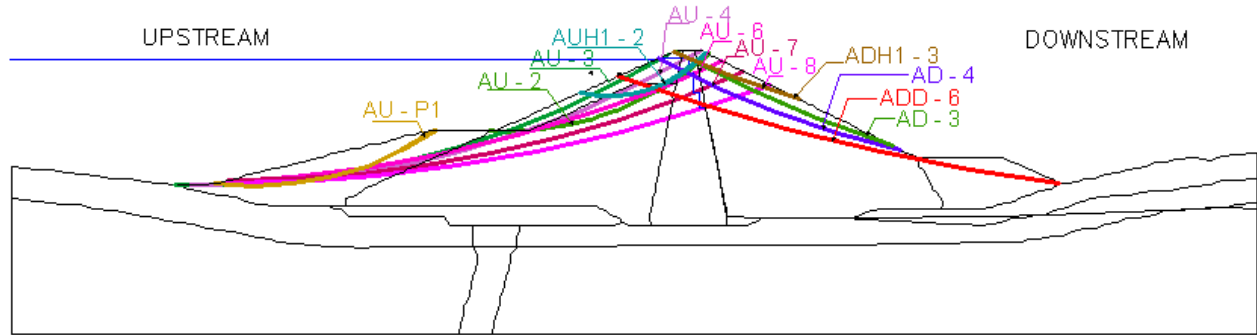


**Figure 12. The twelve slip surfaces that were examined for the main cross section of figure 2**

Anelastic (permanent) displacements using the approach of Makdisi [3] were calculated based on the diagrams of Figure 13 that were proposed for earth and rockfill dams as well as embankments, as long as the following conditions are valid: a) the earthquake is of magnitude less than 8, b) the freeboard is at least 1m, c) there are not features that are vulnerable to small deformations and d) the materials filling dam body and foundation are not prone to liquefy. In our case, all the above conditions do apply since a) following the attenuation relationships of Ambraseys [16], Skarlatoudis [17] and Spudich [18], a magnitude of almost 7.5 is obtained for an earthquake with peak ground acceleration of 0.37g at an epicentral distance of 10km, b) the freeboard is 7m and c) based on laboratory tests results, it has been concluded that soil materials of shell and rockfill, neither behave strongly non-linear in the major part of the dam, nor are susceptible to liquefaction.

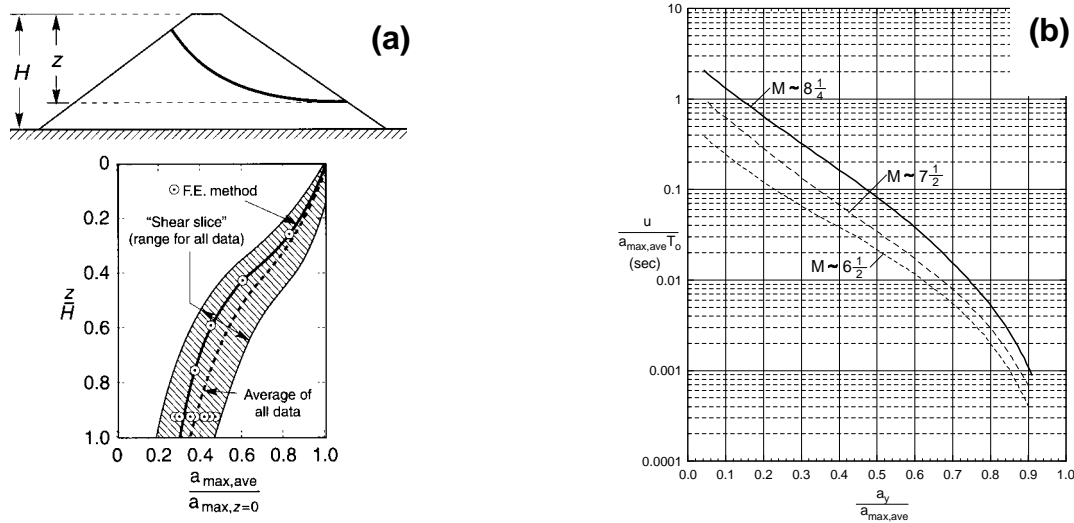


**Figure 13. Makdisi [3]: (a) Variation of maximum acceleration ratio with depth of sliding mass (b) variation of yield acceleration with average normalized displacement.**

To apply Makdisi [3] methodology, the maximum peak acceleration  $A_{\max,ave}$  has to be defined. This is obtained as the average over the computed peak accelerations of the elements inside the sliding block from 2D response analysis described in the previous section. Nevertheless, having in mind that all these peak accelerations do not occur simultaneously, instead of the  $A_{\max,ave}$ , the effective peak acceleration determined as  $A_{eff,ave} = 0.75A_{\max,ave}$  has been used. Together with the first natural period of vibration of the dam for each input motion used,  $T_{o,seis}$ , the expected anelastic displacements at the potential slip surfaces can be obtained from the diagram of figure 13b. An example is given in Table 5 for the Aegio Earthquake (No 2 in table 3).

**Table 5. An example of the application of Makdisi [3] methodology**

AEGIO ROCK		Slip surface	Yield $A_y$ (g)	Maximum $A_{\max,ave}$ (g)	Effective $A_{eff,ave}$ (g)	$X=A_y/A_{eff}$	$Y=u/A_{eff}T_o$	$u_{eff}$ (cm)
$T_{o,seis}$ (sec)		auh1-2	0,237	0,937	0,703	0,337	0,1022	<b>88</b>
1,25	upstream	au-2	0,173	0,763	0,572	0,302	0,1311	<b>92</b>
		au-3	0,165	0,716	0,537	0,307	0,1267	<b>83</b>
		au-4	0,169	0,765	0,574	0,295	0,1391	<b>98</b>
		au-6	0,176	0,776	0,582	0,302	0,1312	<b>94</b>
		au-7	0,218	0,649	0,487	0,448	0,0503	<b>30</b>
		au-8	0,253	0,563	0,423	0,599	0,0160	<b>8</b>
		au-p1	0,134	0,742	0,557	0,241	0,2107	<b>144</b>
	downstream	adh1-3	0,313	0,765	0,574	0,546	0,0242	<b>17</b>
		ad-3	0,273	0,723	0,542	0,503	0,0339	<b>23</b>
		ad-4	0,283	0,710	0,532	0,532	0,0272	<b>18</b>
		add-6	0,300	0,697	0,523	0,574	0,0193	<b>12</b>

A synopsis of the expected anelastic displacements for a number of potential slip surfaces examined in this case study and for the design assumptions mentioned in the previous section is given in Table 6. It is obvious that upstream slip surfaces suffer larger displacements than downstream ones, a fact that was expected taking into account accelerations needed to cause incipient movement. It is also observed that, independently of the design parameters used in 2D analyses, largest permanent displacements are observed for No 2 input motion (Aegio earthquake). This observation is consistent with the results of the

**Table 6. Synopsis of expected anelastic displacements using Makdisi [3] methodology**

		$G_{o,des}$				$G_{o,max}$				$G_{o,min}$			
		1	2	3	4	1	2	3	4	1	2	3	4
	Slip surface	$u_{eff}$ (cm)	$u_{eff}$ (cm)	$u_{eff}$ (cm)	$u_{eff}$ (cm)	$u_{eff}$ (cm)	$u_{eff}$ (cm)	$u_{eff}$ (cm)	$u_{eff}$ (cm)	$u_{eff}$ (cm)	$u_{eff}$ (cm)	$u_{eff}$ (cm)	$u_{eff}$ (cm)
upstream	AUH1-2	16	88	30	17	7	128	26	16	<1	36	10	8
	AU-2	27	92	44	32	19	135	39	28	4	53	21	16
	AU-3	27	83	74	61	26	112	43	46	11	76	42	28
	AU-4	28	98	63	48	23	134	43	39	6	70	32	23
	AU-6	23	94	49	40	18	133	40	32	5	55	22	17
	AU-7	6	30	15	11	5	53	15	10	<1	12	5	3
	AU-8	<1	8	5	3	<1	22	5	3	<1	3	<1	<1
downstream	AU-P1	42	144	144	133	45	147	87	111	34	180	61	51
	ADH1-3	<1	17	5	4	<1	33	7	3	<1	9	<1	<1
	AD-3	3	23	10	6	<1	30	18	5	<1	13	6	4
	AD-4	<1	18	7	4	<1	26	12	3	<1	8	<1	<1
	ADD-6	<1	12	4	<1	<1	17	6	<1	<1	4	<1	<1

2D response analysis where maximum values of peak acceleration are detected for this input motion.

The most critical slip surface in terms of largest computed anelastic displacements is AU-P1, but it is not considered critical for the serviceability integrity of the dam since it has a local shallow character spatially restricted at the protective upstream side fill. AUH1-2, AU-2, AU-3, AU-4 and AU-6 slip surfaces seem to experience large anelastic displacements (33, 43, 52, 51 and 44 cm per overall average, respectively). AU-3 is very shallow going through the rockfill cover of the dam's shell and extending till the foot of the side shell, while AUH1-2, AU-2, AU-4 and AU-6 are passing through dam's core with AUH1-2 and AU-2 having a local character ending within dam's shell (AUH1-2) and at the top of the interface between the shell and the side fill (AU-2). Those slip surfaces passing through the clayey core of the dam are considered the most critical ones for the serviceability and safety of the dam.

Given that Makdisi [3] approach has been validated with measurements of anelastic displacements from dams and embankments lower than 60-70m of height and it is based on an average effective peak acceleration without considering other characteristics of an acceleration time history, (e.g. number of cycles exceeding yield acceleration, duration), additional computations were made based on an average acceleration time history from the elements that intersect with each slip surface (Figure 14a), based on which Newmark's [4] approach is applied considering the sliding mass as a rigid block (TNMN [15]). This average acceleration time history  $K_{av}(t)$  is defined as the ratio of the sum of the horizontal forces that act at the slip surface,  $F(t)$ , over the total mass of the sliding block according to the following relationships.

$$K_{av}(t) = \frac{F(t)}{m} \quad F(t) = \sum_{i=1}^n [\tau_{hvi}(t).L_i + \sigma_{hi}(t).d_i]$$

Expected anelastic displacements are determined with double integration of those parts of the average acceleration time history that exceed yield acceleration corresponding to a specific potential slip surface (Figure 14b). Additional computations were performed only at those slip surfaces that were considered the most critical ones, either because they undergo large permanent displacements or are essential for the safety and integrity of the dam. Table 7 summarizes the results of anelastic displacements for the examined, with this approach, slip surfaces. The largest permanent displacements are now observed for No 4 input motion (Table 3) independently of the design parameters used in 2D analyses, although maximum peak accelerations of average time histories are again observed for No 2 input motion. Meaning that other parameter, such as duration of input motion with respect to the number of cycles exceeding yield acceleration, than maximum acceleration value, mostly affect the level of anelastic

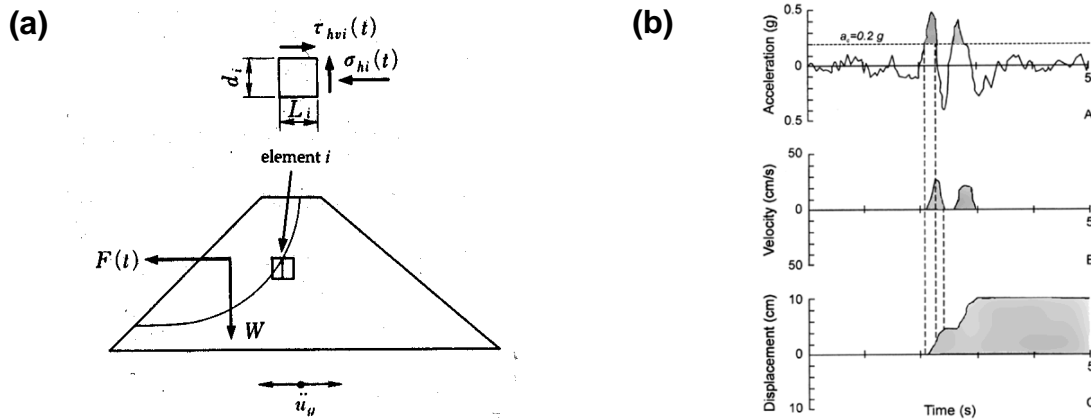


**Figure 14. a) Calculation of average acceleration time history along the slip surface b) Calculation of permanent displacements according to Newmark [4].**

**Table 7. Synopsis of expected anelastic displacements using Newmark's [4] approach with the use of an average acceleration time history**

		$G_o$				$G_{max}$				$G_{min}$			
	Slip surface	1	2	3	4	1	2	3	4	1	2	3	4
		$U_{eff}$ (cm)	$U_{eff}$ (cm)	$U_{eff}$ (cm)	$U_{eff}$ (cm)	$U_{eff}$ (cm)	$U_{eff}$ (cm)	$U_{eff}$ (cm)	$U_{eff}$ (cm)	$U_{eff}$ (cm)	$U_{eff}$ (cm)	$U_{eff}$ (cm)	$U_{eff}$ (cm)
upstream	AUH1-2	51	90	57	88	18	119	69	135	1	37	15	69
	AU-2	60	71	43	98	20	109	65	145	1	27	8	51
	AU-4	9	37	30	33	10	44	24	31	1	13	1	15
	AU-7	2	10	4	7	2	29	5	11	0	1	0	1
	AU-P1	17	82	86	127	29	105	80	96	12	44	26	75

displacements in this approach. An example is given in Figure 15 for AU-2 slip surface,  $G_{o,des}$  assumption and input motion No2 (left) and No4 (right). Yield acceleration for AU-2 slip surface is 0.173g, while peak acceleration of the average time histories (top of figure) is almost 0.9g and 0.6g for No2 and No4 respectively. In case of No2 analysis, that part of the average time history that exceeds yield acceleration has duration of almost 3sec (left) in large contrast with No4 one (right), where the respective part has 13sec duration and resulted at 71cm and 98cm of permanent displacement respectively (bottom), despite the strong difference in the level of their peak values.

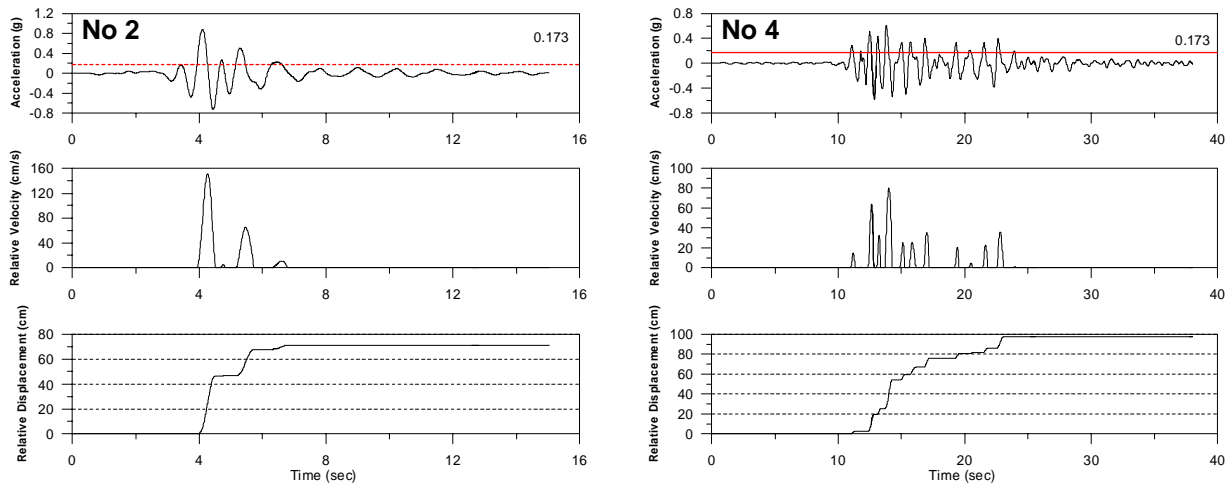


**Figure 15. Average acceleration time (top) and relative displacement (bottom) for AU-2 slip surface,  $G_{o,des}$  assumption for No 2 (left) and No 4 (right) earthquakes**

## CONSEQUENCES OF INDUCED DISPLACEMENTS ON SEISMIC SAFETY OF THE DAM

The most important consequences of the sliding movements and the seismic settlements produced by the safety evaluation earthquake (SEE) are discussed in the next paragraphs.

### Seismic Settlements

There are several ways to calculate seismic settlements of a dam, according to relevant bibliography. In this case, seismic settlements of the dam are based on an empirical relationship where the product of a seismic energy factor (SEF) and a resonance factor (RF) are expressed as a percentage of the dam's body and the foundation compressible soil layers height (in this case, settlements of the rocky subsurface, are considered as practically null). Seismic energy factor (SEF) depends on earthquake magnitude (M) and horizontal peak ground acceleration (PGA), while resonance factor (RF) is dependent on the dam type and the distance between the source of seismic energy release and the dam site (Swaigood [19]). A crude



approximation of the maximum seismic settlement via this empirical manner is 25 cm exclusively attributed to dam's body settlements, since rock formations are practically incompressible.

### **Reduction of freeboard**

The earthquake - induced displacements, as calculated via decoupled analyses, do not exceed 1.5m, under any circumstances examined (most unfavorable combination of frequency content of the input motion combined with the most critical potential sliding mass and the most troublesome values concerning materials and foundation shear modulus at low strains). Superposed values of anelastic displacements and seismic settlements are not deemed to exceed the extreme value of 1.7m, which already is believed to be an absolute upper limit. Therefore, the largest reduction of the freeboard due to a potential sliding displacement of an upstream deeper block cutting through the whole width of the clayey core was estimated in an extreme case of the order of 1.6m. The crest level is located at +410.0m altitude the future full reservoir level at +403.0m and the upper core level at +406.5m. Therefore, after the SEE, the top of the core would drop at +404.9m and the crest level at +408.4m. As a consequence, the top of the core would still be 1.9m above the new full reservoir level and the total freeboard with respect to the crest level would still be about 5.4m. Obviously, the reservoir water will not overflow the dam even in this extreme condition.

### **Risk of internal erosion**

Another important issue is the problem of internal erosion after a strike of the SEE. According to the recent Swiss Guidelines [8], the expected displacements should not exceed about 50% of the combined thickness of the coarse and fine-grained upstream or downstream filters. The maximum expected permanent displacement along a slip surface cutting across the filters upstream and downstream at a depth less than 25m, would not exceed 1.5m, which represents about 20% of the combined thickness of filters and drainage layers. For slip surfaces deeper than 30m, the maximum expected anelastic displacements do not exceed 1m, representing thus a percentage of almost 25% of the combined thickness of filters and drainage layers. In any case, the integrity of filters should be adequate, even after the earthquake – induced permanent movements resulting from the SEE strike. Moreover, core material disposes self-healing properties, ensuring that no concentrated leak is prone to develop along the potential slip surface.

## **CONCLUSIONS**

The main conclusions of this project can be drawn as follows:

- The methodology adopted to investigate seismic integrity of a 130m high rockfill dam with a central clayey core resting on phyllites and limestones, for the safety evaluation earthquake (SEE), is a 2-D plane strain FE analysis of three different cross sections. Non-linear behavior of dam and foundation material was approximated by equivalent linear procedure with an hysteretic type of damping. All of three cross sections were excited by four different accelerograms, carefully chosen with respect to seismotectonic and local conditions of the dam site, and were normalized at 0.37g, a peak ground acceleration corresponding to rock outcrop conditions and a mean return period of 10000 years.
- Permanent displacements calculated were based on two different decoupled analyses. The largest anelastic displacements during the SEE might reach values of the order of 1.5m, considered already as an extreme case. On top of those permanent movements, seismic settlements, roughly estimated of the order of 0.25m as a maximum value, are added.
- Safety against overflow is adequate, even after freeboard reduction calculated for SEE and for a worst case scenario.
- The filters, upstream and downstream satisfy completely New Swiss Seismic Guidelines and will perform sufficiently, even after the SEE earthquake-induced sliding displacements.

## ACKNOWLEDGEMENTS

The authors would like to greatly acknowledge the Greek Public Electricity Company for the assignment and funding of the present project and also for permission of publication of its main results. Prof. E. Comodromos is greatly appreciated for his scientific contribution.

## REFERENCES

1. Wieland, M., Malla, S. "Seismic Safety evaluation of a 117m high embankment dam resting on a thick soil layer." Proc of 12<sup>th</sup> European Conference of Earthquake Engineering, 2002. CDRom paper No.128.
2. Cascone, E., Rampello, S. "Decoupled seismic analysis of an earth dam." Soil Dynamics and Earthquake Engineering, 2003; 23: 349-365.
3. Makdisi F. I., Seed, H. B. "Simplified procedure for estimating dam and embankment earthquake-induced deformations." Journal of the Geotechnical Engineering Division, ASCE 1978; 104(GT7): 849-867.
4. Newmark, N.M. "Effect of earthquakes on dams and embankments." Geotechnique 1965; 15(2):
5. Gazetas, G. "Lesson Handouts on Soil Dynamics (in greek)". Geotechnical Division, School of Civil Engineering, National Technical University of Athens, 1995.
6. Das, B. M. "Principles of Soil Dynamics." Boston: PWS-KENT Publishing Company, 1993
7. Seed, H. B., Booker, J. R. "Stabilization of Potential Liquefiable Sand Deposits Using Gravel Drains." Journal of the Geotechnical Engineering Division 1977; 103(GT7): 757-768
8. Directives de l' OFEG. Securite des ouvrages d' accumulation; Version 1.1, Novembre 2002.
9. Finn, W.D.L., Ledbetter, R.H., Marcuson III, W.F. "North American practice for evaluating the seismic safety of embankment dams." Proceeding of the 1<sup>st</sup> International Conference on Earthquake Geotechnical Engineering, Tokyo, Japan, Ishihara (ed) – A.A. Balkema, 1997; 1: 1227-1252.
10. Design Standards No. 13, Embankment Dams. "Chapter 13: Seismic Design and Analysis", U.S. Bureau of Reclamation (Draft – June 16, 1999).
11. EAK(2000), Greek Seismic Code.
12. EC8 (2002), Design Provisions for Earthquake Resistance of Structures, Part 1-1: General Rules- Seismic Actions and General Requirements for Structures (draft), pren 1998-5, Eur. Committee for Standardization, Brussels.
13. Ambraseys, N., P. Smit, R. Berardi, D. Rinaldis, F. Cotton, C. Berge-Thierry. "Dissemination of European Strong Motion Data". CD-ROM collection, 2000. European Council, Environment and Climate Research Programme.
14. Rathje E.M., N.A. Abrahamson, J.D. Bray. "Simplified frequency content estimates of earthquake ground motions." Journal of Geotechnical & Geoenvironmental Engineering, 1998; 124(2): 150-159.
15. TAGAssoft Limited (1984), Computer Programs TELSTA, TELDYN and TNMN California.
16. Ambraseys, N.N., K.A. Simpson and J.J. Bommer. "Prediction of horizontal response spectra in Europe." Journal of Earthquake Engineering and Structural Dynamics, 1996; 25: 371-400.
17. Skarlatoudis, A.A., Papazachos, B.C., Margaris, B.N., Theodulidis, N., Papaioannou, Ch., Kalogeras, I., Scordilis, E.M., Karakostas, V. "Empirical peak ground-motion predictive relations for shallow earthquakes in Greece." Bulletin of Seismological Society of America, 2003; 93(6): 2591-2603.
18. Spudich, P., W.B. Joyner, A.G. Lindl, D.M. Boore, B.M. Margaris, J. B. Fletcher. "SEA99: A revised ground motion prediction relation for use in extensional tectonic regime." Bulletin of Seismological Society of America, 1998; 89: 1156-1170.
19. Swaisgood J.E. "Seismically-Induced Deformation of Embankment Dams.' Proc of 6th U.S. National Conf.on Eathquake Engineering, May 13- Jun 4, 1998, Seattle.